Unlocking the Power of the Microscale: Insights into CO_2 Mineralization through Microanalysis

Introduction

Geologic CO_2 sequestration through mineralization is a climate change mitigation strategy that provides secure CO_2 storage over geologic time scales. Raza et al. (2022) summarized several studies that successfully demonstrated its applicability at pilot scales (e.g., Carbfix in Hellisheiði, Iceland and Wallula in Washington, US).

Several studies investigated the kinetics of this process, however many of them analysed the reaction in pulverized rocks, thereby presenting scenarios that are different from those encountered in subsurface formations. Different steps in CO2 mineralization are significantly governed by available fluid pathways and influenced by pore-size distribution, feedback mechanisms and permeability alteration (Steinwinder & Beckingham, 2019; Zachara et al., 2016). Therefore, accurate estimation of CO_2 uptake in subsurface basalt mandates obtaining high-resolution, high-quality images that can effectively characterise the reaction progression.

The advancement of image-based techniques facilitates the study of the CO_2 mineralization reaction at the nano to micro scales and improves our understanding of the CO_2 sequestration potential in mafic/ultramafic rocks (Fig. 1). We surveyed the applicability of imaging and microanalyses techniques in the study of CO_2 mineralization. X-ray Computed Microtomography (XCT) and Scanning Electron Microscope (SEM) techniques provide insights into pore space evolution as a function of reaction progression. Of the surveyed methods, time resolved XCT can provide important insight into the pore space alteration that occurs during mineralization. We used this method to study the CO_2 uptake sequestration potential of ultramafic rocks.

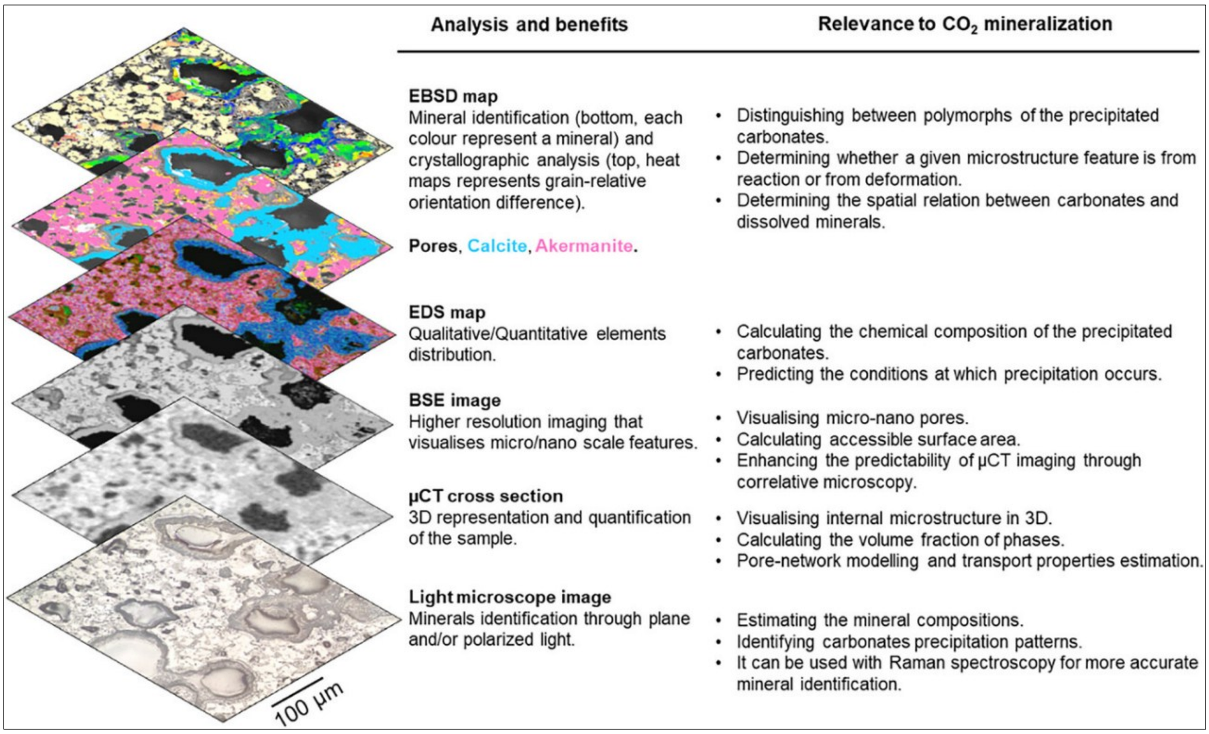

Figure 1. Demonstration of how integrating different imaging techniques helps in understanding different aspects of the CO_2 mineralization process(Khudhur et al., 2026).

Methods

XCT data were collected by utilizing a bespoke X-ray translucent cell developed in-house (Watt et al., 2024). CO_2 saturated fluid can be prepared and injected into the cell using a syringe pump. The temperature of the cell (170 °C) can be controlled via external band heaters, while the pressure can be maintained via a back-pressure regulator. The core sample being investigated (diameter = 1 cm and up to 2 cm height) is housed in the cell and can be carbonated using the prepared CO_2 saturated solution. The specifications of the cell and the experimental setup are described elsewhere (Watt et al., 2024).

Throughout the reaction period, the cell was routinely imaged using XCT, thereby yielding a 4D data (three spatial dimensions + time). Additionally, liquid output samples from the cell were collected for composition analysis. At the end of the experiment, the core was recovered for further analysis using SEM-techniques.

Results

Time-resolved XCT imaging reveals progressive alteration of the basalt microstructure, with regions of dissolution and precipitation being observed during carbonate mineralization. This affects the porosity of the host rock due to fracture generation and/or pore filling (Khudhur et al., 2026; Watt et al., 2025).

CO_2 mineralization can be induced through increasing the alkalinity in the reaction fluid. Post-reaction SEM imaging confirmed the presence of carbonates within the studied sample (Watt et al., 2025).

The composition of the cells effluent correlates with influent chemistry, with higher alkalinity resulting in lower dissolution (Watt et al., 2025).

Conclusions

These observations highlight the value of using 4D imaging in the study of CO_2 mineralization in basalt, to provide information regarding pore space alteration, and in the identification of regions that favour dissolution or precipitation. When combined with other methods (e.g., core flooding for permeability measurement and XRD for mineralogy), 4D data correlated with SEM imaging can provide important information regarding reaction localization and transport control mechanisms. Together, they help in extending lab-scale observations to the field-scale and thus predicting accurate CO_2 uptake.

Acknowledgements

This work was supported by the United Kingdom Research and Innovation-Natural and Environmental Research Council (UKRI-NERC) grant (INCLUSION-grant number NE/X014789/1).

References

Khudhur, F. W. K., Butler, I. B., & Gilfillan, S. M. V. (2026). Small is the New Large: Demonstration of how Microanalyses Elucidate Large-Scale CO $_2$ Uptake Through Mineralization. *Advanced Sustainable Systems*, *10*(2). https://doi.org/10.1002/adsu.202501549

Raza, A., Glatz, G., Gholami, R., Mahmoud, M., & Alafnan, S. (2022). Carbon mineralization and geological storage of CO2 in basalt: Mechanisms and technical challenges. *Earth-Science Reviews*, *229*, 104036. https://doi.org/10.1016/J.EARSCIREV.2022.104036

Steinwinder, J., & Beckingham, L. E. (2019). Role of pore and pore-throat distributions in controlling permeability in heterogeneous mineral dissolution and precipitation scenarios. *Water Resources Research*, *55*(7), 5502–5517. https://doi.org/10.1029/2019WR024793

Watt, I. D., Butler, I. B., Gilgannon, J., Khudhur, F., Molnar, ian L., Fusseis, F., Haszeldine, S., & Gilfillan, S. M. V. (2025). *Experimental Observations that Carbonation of Basalt Stores CO2 in Coupled Reaction Induced Fractures*. https://doi.org/10.2139/ssrn.5281347

Watt, I. D., Butler, I. B., Gilgannon, J., Martins, L., Fusseis, F., Haszeldine, R. S., Molnar, I., & Gilfillan, S. M. V. (2024). X-ray translucent reaction cell for simulation of carbon mineral storage reservoir environments. *International Journal of Greenhouse Gas Control*, *137*, 104195. https://doi.org/10.1016/j.ijggc.2024.104195

Zachara, J., Brantley, S., Chorover, J., Ewing, R., Kerisit, S., Liu, C., Perfect, E., Rother, G., & Stack, A. G. (2016). Internal domains of natural porous media revealed: critical locations for transport, storage, and chemical reaction. *Environmental Science and Technology*, *50*(6), 2811–2829. https://doi.org/10.1021/acs.est.5b05015